33rd Annual International Conference of the IEEE EMBS
Boston, Massachusetts USA, August 30 - September 3, 2011

Reconstructing hand kinematics during reach to grasp movements from electroencephalographic signals

Harshavardhan A. Agashe, *Student member, IEEE* and José L. Contreras-Vidal, *Senior Member, IEEE*

Abstract—**With continued research on brain machine interfaces (BMIs), it is now possible to control prosthetic arm position in space to a high degree of accuracy. However, a reliable decoder to infer the dexterous movements of fingers from brain activity during a natural grasping motion is still to be demonstrated. Here, we present a methodology to accurately predict and reconstruct natural hand kinematics from non-invasively recorded scalp electroencephalographic (EEG) signals during object grasping movements. The high performance of our decoder is attributed to a combination of the correct input space (time-domain amplitude modulation of delta-band smoothed EEG signals) and an optimal subset of EEG electrodes selected using a genetic algorithm. Trajectories of the joint angles were reconstructed for metacarpo-phalangeal (MCP) joints of the fingers as well as the carpo-metacarpal (CMC) and MCP joints of the thumb. High decoding accuracy (Pearson's correlation coefficient, r) between the predicted and observed trajectories ($r = 0.76 \pm 0.01$; averaged across joints) indicate that this technique may be suitable for use with a closed-loop real-time BMI to control grasping motion in prosthetics with high degrees of freedom. This demonstrates the first successful decoding of hand pre-shaping kinematics from noninvasive neural signals.**

I. Introduction

IT is estimated that 541,000 of the 1.6 million amputees in the United States in 2005 were upper limb amputees with 8% (41,000) classified as a major limb loss, i.e., excluding fingers [1]. Needless to say, the quality of life for these individuals may be severely reduced. With the availability of state-of-the-art prosthetics like the 22 degree-of-freedom (DoF) modular prosthetic limb fabricated by John Hopkins University Applied Physics Laboratories (JHUAPL) that has capabilities of human-like dexterity, there is a need for high-performing decoding interfaces that can reliably predict finger movement intentions during ecologically valid situations like grasping objects.

Brain-Machine Interface (BMI) systems for upper limb prosthetics have traditionally focused on predicting arm movement during the transport phase of reach-and-grasp tasks in the form of endpoint trajectories or wrist, elbow and shoulder angles and velocities in monkeys and humans [2-8]. However, to control a functional neuromotor prosthetic, algorithms designed to decode the pre-shaping of the hand in conjunction with the transport are needed. Decoding dexterous finger movement during tasks like grasping and manipulating objects is substantially more complex because of the high DoFs in the human hand.

Studies have investigated classifying finger movements from neural activity [9,10]. Recent studies have shown the possibility of decoding kinematic parameters of movement during individuated finger movements, and simple grasping motion from local motor potentials (LMPs) extracted from electrocorticographic (ECoG) signals in humans [11,12]. Research from intracortical studies in monkeys has shown that it is possible to decode grasp aperture and finger movements during natural grasping motions [13-15]. A high-performing decoder, capable of inferring the coordinated movements of individual finger joints during an ecological grasping situation involving real objects is, however, missing.

BMIs typically use volitional modulation of the power in specific frequency bands by users as control signals to drive movement in prosthetics. Previous work suggests that low-frequency time-domain signals in EEG and ECoG may be a suitable input feature space to decode arm and hand movement. We hypothesize that using the correct input space in combination with an optimal subset of EEG channels will lead to high correlations between predicted and observed trajectories of finger movements during hand pre-shaping to grasp everyday objects; a gap which this study aims to fill.

In this study we demonstrate the design of neural decoders using low-pass filtered EEG signals as inputs. The subset of EEG electrodes leading to an optimal decoding is found using a genetic algorithm (GA). EEG and hand kinematics were simultaneously recorded from five healthy individuals while they reached and grasped one of five objects kept in front of them. Predicted trajectories were compared with observed trajectories for the (four) finger MCP, thumb MCP and thumb CMC joint angles.

II. Methods

A. Experiment design and data acquisition

Five healthy right-handed subjects participated in this study after giving informed consent approved by the Institutional Review Board at the University of Maryland-College Park. EEG and hand kinematics were recorded

Manuscript received April 15, 2011. This work was supported in part by a Kinesiology GRIP research award to H.A.A. and by the National Institutes of Health under grant P01 HD064653.

H. A. Agashe is with the Graduate Program in Neuroscience and Cognitive Science, and Department of Kinesiology, University of Maryland, College Park, MD 20742 USA (corresponding author, email: agashe@umd.edu).

J. L. Contreras-Vidal is with Department of Kinesiology, Fischell Department of Bioengineering, and Graduate Program in Neuroscience and Cognitive Science, University of Maryland, College Park MD 20742 USA. (e-mail: pepeum@umd.edu).

simultaneously while subjects performed a grasping task. Subjects were seated behind a table with five objects (calculator, CD, espresso cup, zipper and a beer mug) arranged in front of them in a semicircle with an approximate radius of 30 cm. The initial position of the hand was palm down and flat on the table at the center of the semicircle. We chose the five objects in our study so as to sample the grasp space evenly based on a prior study that documented the distribution of static postures of grasp for 57 imagined everyday objects [16]. On the presentation of an auditory 'go' cue (100 ms tone at 2 kHz) subjects were instructed to select, reach out and grasp any of the five objects. Subjects kept a steady grasp on the objects until an auditory 'stop' cue (200 ms tone at 1 kHz) was presented 5 s after the 'go' cue, on hearing which they returned their hand to the resting initial position. The time until the presentation of the 'go' cue for the next trial was Gaussian distributed with a mean of 7 s and standard deviation of 1 s. Five blocks of 12 minutes each were recorded for subjects S1,S2 and S3 and four blocks were recorded for subjects S4 and S5. 50 trials were recorded in each block on average. At the end of each block, the placement of the five objects was rotated clockwise so as to provide a plurality of reach directions for grasping the same object, ensuring that eye movements did not play a role in decoding.

Whole head EEG was recorded using a 64 channel cap, amplified and digitized at 500 Hz with a Net Amps 300 acquisition system (Electrical Geodesics Inc.). The trajectories of 23 joint angles were recorded with a wireless data glove (CyberGlove, Immersion Inc.) at a resolution of 0.93° at a non-uniform sampling rate of 35-70 Hz.

B. Preprocessing

All analyses were performed using custom built programs in MATLAB (Mathworks Inc.). The raw synchronized EEG and kinematics were down-sampled to 100 Hz following the application of a Chebychev type-II antialiasing filter at 40 Hz. The raw kinematics were interpolated with a piecewise cubic hermite interpolating polynomial and up-sampled to 100 Hz. After rejecting 18 peripheral EEG channels and channels with high impedances (greater than 200 kΩ), EEG was re-referenced to a common average (CAR). EEG was

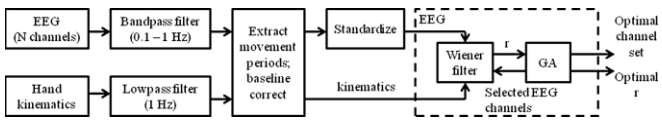

Fig. 1. Flowchart showing the decoder block diagram. Preprocessed EEG and kinematics is passed to the decoder module (dotted box), containing the linear decoder and the GA wrapper. The GA maximizes the correlation coefficient (r) between the observed and predicted kinematics.

then high pass filtered at 0.1 Hz with a zero-phase 4th order Butterworth filter. Next, both EEG and kinematics were low-pass filtered at 1 Hz with a zero-phase 1st order Butterworth filter. All EEG channels were standardized by their respective means and standard deviations. The continuous EEG and kinematics were segmented into trials consisting of the movement period from 0.5 s before movement onset to 2.5 s after movement onset. Any data outside of the movement periods were discarded. The segmentation was done to provide a balanced representation of movement and rest periods for the purpose of training the decoder. Movement onsets were determined to be points at which the joint angle speed exceeded 5% of the maximum during a trial for the first time. The segmented data were baseline corrected using a baseline of -0.5 s to 0 s with respect to movement onset.

C. Linear decoding model

The decoding approach is depicted in Fig. 1. EEG channels to be used for decoding were selected based on an evolutionary optimization procedure (described in the next section). Each of the movement variables was independently modeled as a linear combination of data from the selected sensors:

$$y[t] = \beta_0 + \sum_{i \in \Psi} \beta_i S_i[t + \Delta]$$

where $y[t]$ is the joint angle time-series being decoded at time t, β_i are the model parameters, S_i are the sensor values for the ith sensor, Δ denotes the time delay (lag) between EEG and kinematics and Ψ is the optimal set of EEG sensors. Model parameters were calculated using the Generalized Linear Model (GLM) framework. The model was validated using 10-fold cross-validation as follows: the data was partitioned into 10 distinct sets. Model parameters were calculated using the first 9 sets (training sets) and its performance tested on the 10th, unseen set (test set). This procedure was repeated with each of 10 sets used as a test set. The predictive power of the decoding model (decoding accuracy) was designated to be the median value of the Pearson correlation coefficient (r) between the observed and predicted kinematics across the 10 folds.

D. Selection of optimal sensors

To optimize the neural decoder, we employed a genetic algorithm to select the EEG channels to be used as inputs to the linear decoder. The genetic algorithm is a search heuristic that is inspired by the process of natural evolution, and which provides a global optimization strategy to search the input space in a directed manner. The first generation was initialized to a population of 22 'individuals' with randomly chosen EEG channels. The fitness of each individual, defined as the median decoding accuracy across the 10 cross validation folds, was evaluated. The 2 best individuals in the population were selected to survive to the next generation unchanged. 16 individuals in the next generation were created using crossovers between the individuals of the current generation. The remaining 4 individuals were mutated from individuals in the current generation. The mutation rate was set to an average of 2 channels in each individual. The algorithm was allowed to run for 500 generations.

III. Results

The decoding accuracy was calculated for the finger MCP, thumb MCP and thumb CMC joints angles by applying the linear decoder at specific lags. The lags were systematically varied from -500 to 0 ms, in steps of 100 ms, so that past brain activity predicted current kinematics. For a specific kinematic variable and lag, decoding accuracy was calculated for each subject and block using the optimal set of EEG sensors as found by the genetic algorithm. Fig. 2 shows an example of the dramatic improvement in decoding accuracy over generations during an optimization run with the GA. In the initial stages, the channel selection is random, but soon converges onto an optimal subset. It can be seen that the decoding accuracy increases correspondingly.

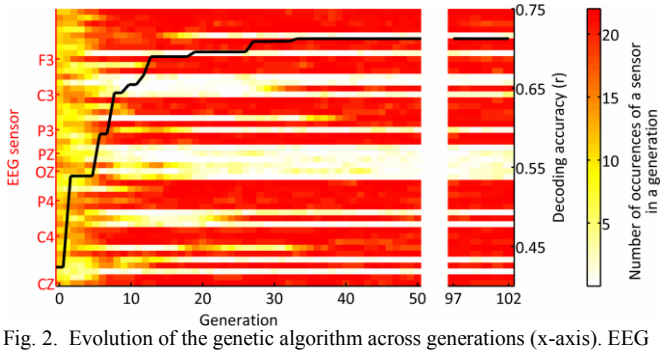

Fig. 2. Evolution of the genetic algorithm across generations (x-axis). EEG channels are shown along the y-axis. Selectivity of channels across individuals in a generation is color coded. At the onset of the optimization, channels are chosen randomly (low selectivity) but quickly converge onto a subset of channels (high selectivity channels), which gives the optimal decoding accuracy. The black trace shows the improvement in the decoding accuracy as the algorithm converges.

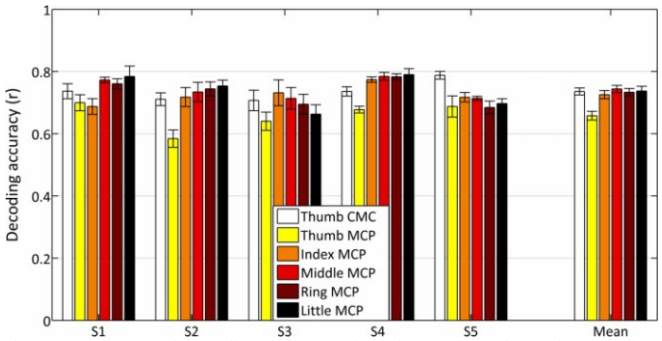

Fig. 3. Summary of decoding accuracy for joint angle and angular velocity prediction. The first five bar groups show the correlation coefficient r (± s.e.m) between the observed and predicted trajectories for each subject; the sixth group shown the mean across all subjects.

Fig. 3 summarizes the decoding accuracies across subjects. The decoding accuracies shown represent mean values calculated using the optimal lag for each subject and block. The decoding accuracies across the entire experiment (all subjects, blocks, lags and kinematic variables) were highly significant ($p<0.001$, Bonferroni corrected for multiple comparisons across all experimental conditions). A kinematic parameter of functional significance is the grip aperture. The maximum grip aperture (MGA) has been shown to scale with the object size [17]. We approximated the grip aperture to a first order as the sum of thumb rotation and index MCP joint angles. The reconstructed trajectories for this approximation are shown in Fig. 4.

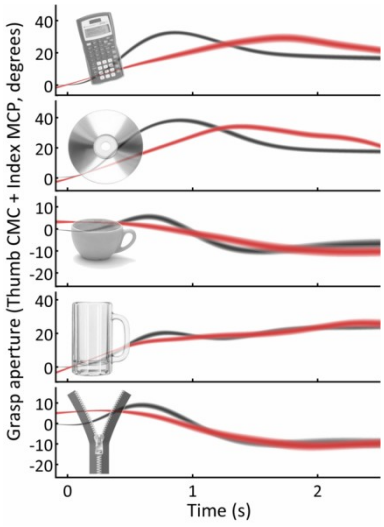

Fig. 4. Average decoded grasp aperture trajectories for subject S1. Observed (black) and reconstructed (red) trajectories are shown for the grasp aperture, approximated as the sum of thumb rotation and index finger MCP. Trajectories for each of the five objects (from top to bottom: calculator, CD, espresso cup, beer mug, zipper) are shown. The width of each trajectory band represents the 90% confidence interval obtained by fitting the data with a Gaussian at each time instant.

Qualitatively, the average MGA, as defined previously, scaled with object size. Moreover, predicted final grip aperture compared well with the measured finger aperture. Interestingly, the timing of peak aperture occurred later for the decoded trajectories compared with the measurements. This is not surprising given that only a single optimal lag was used by the decoder for prediction, and that our working definition of MGA was not based on the distance between the endpoints of the index and thumb, but rather on proxies based on the angular position of those figures at the most proximal joint.

IV. Discussion

This study demonstrates the feasibility of inferring the kinematics of natural reach-to-grasp movements, with a suitable choice of the input feature space and optimization over EEG channel subsets with high accuracy. Previous studies have investigated decoding the stereotypical opening and closing motion of the hand, or movements of individuated fingers, tasks that arguably are not used in day-to-day life [11,12]. The task in this study involved making a decision to select an object, planning the goal of the movement, programming the movement, and executing the grasp in conjunction with specification of the appropriate hand transport trajectory. Previous studies have shown the involvement of multiple cortical areas in such tasks [2,18,19]. The use of EEG affords a global view of the brain activity at the macroscopic level and is thus well suited for this task. A summary of earlier results pertaining to decoding finger kinematics from neural activity is provided in Table 1, along with our results for comparison.

We are cognizant that EEG is susceptible to various artifacts, the most prominent being eye movement, blinking and muscle artifacts [20]. Notably, our preprocessing methods did not use any artifact rejection techniques. In this regard, our results are robust against artifacts, as the prediction accuracies were high despite the data used for training and testing the model containing artifacts. While eye movements may correlate with the hand position, it is unlikely that they correlate with finger joint angle

trajectories. Nonetheless, to conclusively discount eye movement as a predictor of grasp trajectories, we changed the placement of objects after each block. This ensured that the direction and view of hand transport for an object was different in each block while the grasp trajectory (but not its gaze-centered view) remained the same. Muscle activity artifacts in the EEG are unlikely to affect our results, since the data was low-pass filtered at 1 Hz prior to decoding, and muscle artifacts are known to contaminate higher frequencies in the theta band and beyond [21].

TABLE I
Summary of decoding accuracy studies

Hand motion	Decoded kinematics	Decoding accuracy	Notes	Refer-ence
Opening and closing hand	Principal component	r = 0.51	Human ECoG	[12]
Finger tapping	MCP joint angles	r = 0.52	Human ECoG	[11]
Object grasping	Grasp aperture	r = 0.62	Monkey LFP	[14]
Object grasping	Finger joint angles	r = 0.74	Monkey multi unit activity	[13]
Object grasping	**MCP joint angles**	**r = 0.76**	**Human EEG**	*

* Current study

While this study successfully used a low-frequency time-domain feature space, there may exist other feature spaces that can contribute to natural movement decoding [22]. Studies have also shown the improvement in decoding accuracies by using multiple lags as inputs to decode movement [3]. The successful use of the genetic algorithm in this study to select relevant EEG channels at a specified lag may be extended to find an optimal feature set from a wide list of features like time-frequency information and simultaneous multiple lags that could maximize decoding of dexterous movements of varying speeds and complexities.

In summary, we propose a new approach to designing EEG-based decoders that can accurately reconstructed finger and thumb joint angles during a reach-to grasp task. To our knowledge, there have been no previous attempts to decode continuous dexterous finger movements from EEG during an ecological grasping task. We believe that the critical factors which result in the successful decoding in this study was use of a suitable input feature space coupled with an optimal subset of EEG channels.

REFERENCES

[1] K. Ziegler-Graham, E.J. MacKenzie, P.L. Ephraim, T.G. Travison, and R. Brookmeyer, "Estimating the prevalence of limb loss in the United States: 2005 to 2050," *Archives of physical medicine and rehabilitation*, vol. 89, 2008

[2] J.M. Carmena, M.A. Lebedev, R.E. Crist, J.E. O'Doherty, D.M. Santucci, D.F. Dimitrov, P.G. Patil, C.S. Henriquez, and M.A.L. Nicolelis, "Learning to control a brain-machine interface for reaching and grasping by primates," *PLoS biology*, vol. 1, Nov. 2003

[3] T.J. Bradberry, R. Gentili, and J.L. Contreras-Vidal, "Reconstructing three-dimensional hand movements from noninvasive electroencephalographic signals," *J. Neurosci.*, vol. 30, Mar. 2010

[4] L.R. Hochberg, M.D. Serruya, G.M. Friehs, J. a Mukand, M. Saleh, A.H. Caplan, A. Branner, D. Chen, R.D. Penn, and J.P. Donoghue, "Neuronal ensemble control of prosthetic devices by a human with tetraplegia.," *Nature*, vol. 442, Jul. 2006

[5] S. Waldert, H. Preissl, E. Demandt, C. Braun, N. Birbaumer, A. Aertsen, and C. Mehring, "Hand movement direction decoded from MEG and EEG.," *J. Neurosci.*, vol. 28, Jan. 2008

[6] J. Wessberg, C. Stambaugh, J. Kralik, P. Beck, M. Laubach, J. Chapin, J. Kim, S. Biggs, M. Srinivasan, and M. Nicolelis, "Real-time prediction of hand trajectory by ensembles of cortical neurons in primates," *Nature*, vol. 408, 2000

[7] A. Georgopoulos, F. Langheim, A. Leuthold, and A. Merkle, "Magnetoencephalographic signals predict movement trajectory in space.," *Experimental brain research*, vol. 167, Nov. 2005

[8] M. Velliste, S. Perel, M.C. Spalding, A.S. Whitford, and A.B. Schwartz, "Cortical control of a prosthetic arm for self-feeding.," *Nature*, vol. 453, Jun. 2008

[9] S.B. Hamed, M.H. Schieber, and a Pouget, "Decoding M1 neurons during multiple finger movements.," *J. Neurophysiol.*, vol. 98, Jul. 2007

[10] V. Aggarwal, S. Acharya, F. Tenore, H.-C. Shin, R. Etienne-Cummings, M.H. Schieber, and N.V. Thakor, "Asynchronous Decoding of Dexterous Finger Movements Using M1 Neurons," *Neural Systems and Rehabilitation Engineering, IEEE Transactions on*, vol. 16, 2008

[11] J. Kubánek, K.J. Miller, J.G. Ojemann, J.R. Wolpaw, and G. Schalk, "Decoding flexion of individual fingers using electrocorticographic signals in humans," *J. Neural Eng.*, vol. 6, 2009

[12] S. Acharya, M.S. Fifer, H.L. Benz, N.E. Crone, and N.V. Thakor, "Electrocorticographic amplitude predicts finger positions during slow grasping motions of the hand.," *J. Neural Eng.*, vol. 7, May. 2010

[13] C.E. Vargas-Irwin, G. Shakhnarovich, P. Yadollahpour, J.M.K. Mislow, M.J. Black, and J.P. Donoghue, "Decoding Complete Reach and Grasp Actions from Local Primary Motor Cortex Populations," *J. Neurosci.*, vol. 30, Jul. 2010

[14] J. Zhuang, W. Truccolo, C. Vargas-Irwin, and J.P. Donoghue, "Decoding 3-D reach and grasp kinematics from high-frequency local field potentials in primate primary motor cortex.," *IEEE transactions on bio-medical engineering*, vol. 57, Jul. 2010

[15] P.K. Artemiadis, G. Shakhnarovich, C. Vargas-Irwin, J.P. Donoghue, and M.J. Black, "Decoding grasp aperture from motor-cortical population activity," *Neural Engineering, 2007. CNE'07. 3rd International IEEE/EMBS Conference on*, 2007

[16] M. Santello, M. Flanders, and J.F. Soechting, "Postural hand synergies for tool use," *J. Neurosci.*, vol. 18, 1998

[17] M. Jeannerod (1981) Intersegmental coordination during reaching at natural objects. In: Long J, Baddeley A (eds) Attention and performance, vol IX. Erlbaum, Hillsdale, NJ, pp 153–169

[18] P. Cisek and J.F. Kalaska, "Neural correlates of reaching decisions in dorsal premotor cortex: specification of multiple direction choices and final selection of action.," *Neuron*, vol. 45, Mar. 2005

[19] T. Ball, A. Schulze-Bonhage, A. Aertsen, and C. Mehring, "Differential representation of arm movement direction in relation to cortical anatomy and function.," *J. Neural Eng.*, vol. 6, Feb. 2009

[20] M. Fatourechi, A. Bashashati, R.K. Ward, and G.E. Birch, "EMG and EOG artifacts in brain computer interface systems: A survey.," *Clinical Neurophysiology*, vol. 118, Mar. 2007

[21] I. I. Goncharova, D. J. McFarland, J. R. Vaughan and J. R. Wolpaw, "EMG contamination of EEG: spectral and topographical characteristics," Clin Neurophysiol, 114: 1580-1593, 2003

[22] N. F. Ince, R. Gupta, S. Arica, A. H. Tewfik, J. Ashe and G. Pellizzer, "High accuracy decoding of movement target direction in non-human primates based on common spatial patterns of local field potentials," PLoS One, 5(12):e14384, 2010